JOURNAL OF APPLIED ELECTROCHEMISTRY 14 (1984) 645–652

The potentiodynamic response of polycrystalline nickel electrodes in 0.5 M K_2CO_3

A. E. BOHÉ, J. R. VILCHE, A. J. ARVÍA

Instituto de Investigaciones Fisicoquímicas Teóricas y Aplicadas (INIFTA), Casilla de Correo 16, Sucursal 4, 1900 La Plata, Argentina

Received 5 September 1983; 19 December 1983

The electrochemical behaviour of nickel in 0.5 M K_2CO_3 is investigated by applying simple and combined potentiodynamic techniques in the potential regions of the $Ni(OH)_2/Ni$ and Ni(III)/Ni(II) redox couples. The diffusion controlled hydrated $NiCO_3$ precipitation interferes with the electroformation of the $Ni(OH)_2$ prepassive layer. Both anodic and cathodic peak multiplicities are observed in the potential range of the Ni(III)/Ni(II) electrode. The presence of CO_3^{2-} ions is tentatively associated with a change in the hydration of the composite $Ni(OH)_2$/NiOOH layer and eventually with HCO_3^- ions coming out from the CO_3^{2-}/HCO_3^- equilibrium, which depends on the local change in pH produced during the corresponding anodic and cathodic reactions.

1. Introduction

In recent years the influence of the electrolyte composition in electrochemical processes has been the subject of particular attention especially in those reactions involving electrodissolution of metals and electroformation of anodic product layers as is the case with nickel in a base [1–13]. The influence of the electrolyte composition in those reactions can be related to:

i. Direct contact metal–ion interaction (adsorption, electrosorption, partial charge transfer)

ii. Competitive water–ion adsorption at the metal surface (modification of the double layer structure at the inner plane)

iii. Interference in the dissolution and precipitation of salts at the metal surface (modification of the double layer structure at the outer plane)

iv. Competitive effect in the formation of the passive oxide layer at the electrode (ionic adsorption at the oxide layer)

v. Change of the chemical composition and structure of the passive oxide layer, including the degree of hydration and crystalline characteristics of the prepassive and passive layers

vi. Change in the electrical conduction properties of the passive layer.

Each one of these aspects either independently or in a combined form should reflect through the electrochemical behaviour of metals in different electrolytes. Unfortunately, the available information in this respect is, at present, rather limited. Nevertheless, metals of the iron group are probably those which have been most extensively studied for practical reasons, although often the corresponding literature is not straightforwardly comparable for an evaluation of the influence of the electrolyte composition on corrosion and passivation. In this sense, recent potentiodynamic data of nickel electrodes in different aqueous media can be optimistically regarded [14, 15].

The present paper refers to the electrochemical behaviour of nickel in potassium carbonate solution at a pH where the influence of the anion can be compared to results obtained in buffered borate–boric acid [13] and in sodium hydroxide–sodium sulphate solutions [16, 17].

2. Experimental details

The experimental set-up was the same as that already described in previous publications [18–21]. Polycrystalline nickel working electrodes ('Specpure', Johnson Matthey Chemicals Ltd) in the form of either fixed wire (0.5 mm diameter;

0021–891X/84 $03.00 + .12

0.25 cm^2 apparent area) or rotating disc (0.07 cm^2 apparent area) axially mounted on a PTFE rod were employed. Electrode potentials were measured against an SCE although potentials in the text are referred to the NHE scale. The reference electrode compartment was connected through a glass stopcock lubricated with the same electrolytic solution and ended with the usual Luggin–Haber capillary tip. A fritted glass disc was also used to prevent the transport of chloride ions from the reference electrode to the bulk electrolyte. The counter-electrode was a large area platinum sheet previously cleaned following conventional procedures.

The nickel electrode pretreatment consisted of an initial mechanical polishing using successively 400 and 600 grade emery papers, and 1 and 0.3 μ grit alumina–acetone suspension, and finally employing the finest grade diamond paste. After polishing the electrode was rinsed in triply-distilled water. Before each measurement the electrode was held for 5 min at -1.0 V, a potential at which net hydrogen evolution occurs. The electrolyte solution (0.5 M K_2CO_3, pH 11.7) was prepared from analytical grade (p.a. Merck) reagent and triply distilled water. Runs were made at 25° C under purified N_2 gas saturation with both still and stirred solutions at different rotation speeds (ω). The electrode was perturbed with single (STPS) and repetitive (RTPS) triangular potential sweeps between preset cathodic ($E_{s,c}$) and anodic ($E_{s,a}$) switching potentials at varying sweep rates v ($0.001\ V\,s^{-1} < v < 10\ V\,s^{-1}$).

3. Results

The potentiodynamic E–i profiles run with the still solution between -0.8 and 1.24 V at $v = 0.25\ V\,s^{-1}$ (Fig. 1) show in the first positive-going potential scan a net anodic current peak at *c.* -0.33 V (Peak I) and in the 0.7–1.0 V range an anodic multiple current peak (Multiplet II) containing at least Peak IIa at *c.* 0.78 V and Peak IIb at 0.87 V, just preceding the oxygen evolution potential region. In this case, Peak IIb is the most relevant. The reverse scan exhibits another composite cathodic peak (Doublet III) in the 0.8–0.6 V range followed by another ill-defined cathodic peak at *c.* 0.58 V (Peak IV). Neither Peak I nor any complementary cathodic current contribution is further noticed after the first positive-going potential scan in the conditions of Fig. 1. These results coincide with those obtained in strong alkaline solutions [16, 17] and in borate–boric acid solutions [13]. Thereby, the RTPS in the following successive potential cycling were limited within the 0.24–1.24 V range.

During RTPS covering the 0.2–1.1 V potential range the relative charge contributions of the components of each multiplet change gradually. Thus, in the second anodic scan Multiplet II presents three well-distinguished contributions located at

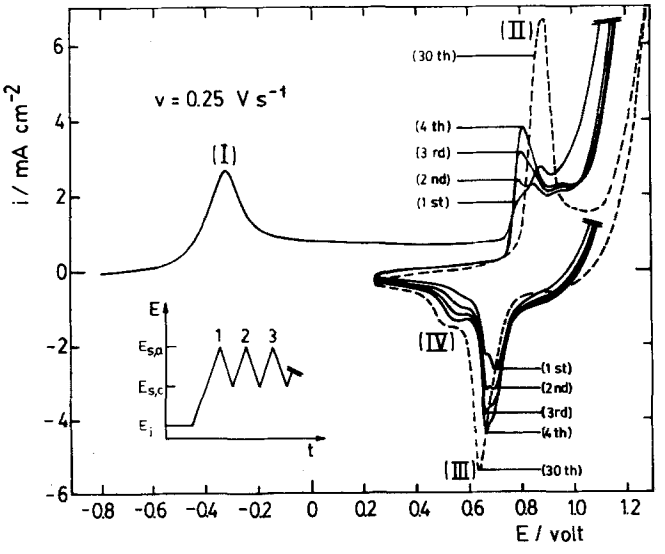

Fig. 1. Potentiodynamic E–I profiles run with still solution at $v = 0.25\ V\,s^{-1}$. The potential programme is depicted in the figure. $E_i = -0.80$ V, $E_{s,c} = 0.24$ V and $E_{s,a} = 1.24$ V. The 1st, 2nd, 3rd, 4th and 5th potential cycles are shown.

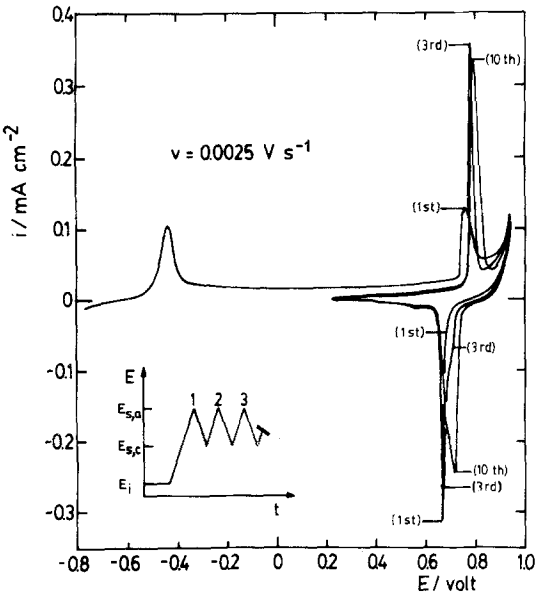

Fig. 2. Potentiodynamic *E–I* profiles run with still solution at $v = 0.0025\ V\ s^{-1}$. The potential programme is depicted in the figure. $E_i = -0.76$ V, $E_{s,c} = 0.24$ V and $E_{s,a} = 0.94$ V. The 1st, 3rd and 10th potential cycles are shown.

0.79 V (Peak IIa), 0.84 V (Peak IIb) and 0.95 V (Peak IIc), but in the 4th anodic scan Peak IIa prevails over Peak IIb, and only a slight contribution of Peak IIc is seen. Finally, after the 30th scan only a single relatively asymmetric peak is formed at 0.88 V (Peak II) whose charge is slightly greater than that observed at the early potential scans. Analogously, during the second cathodic scan the relative contributions of Peak IIIa (at 0.70 V) in Multiplet III decreases at the expenses of Peak IIIb (0.66 V). After 30 cycles, only a single peak appears (Peak III) which is shifted slightly towards more negative potentials. No change can, in principle, be assigned to Peak IV at 0.55 V except that coming from the baseline a shift caused by the decaying portion of Peak III. During cycling the change in cathodic charge is accompanied by the change in anodic charge to keep the anodic to cathodic charge ratio assigned to the $Ni(OH)_2/NiOOH$ couples equal to one. Simultaneously, the polarization of the oxygen evolution reaction increases.

The characteristics of the *E–i* displays are also remarkably dependent on v. Thus, at $v = 0.0025\ V\ s^{-1}$ (Fig. 2) the charge increase observed during the potential cycling is accompanied by changes in both their relative distribution and the potential ranges of the processes associated with both the composite anodic and cathodic multiplets. During the potential cycling these multiplets move slightly towards more positive potentials, and simultaneously, the current components located at the positive potential side become appreciably enhanced. But in this case, the *E–i* profile in the potential range of the oxygen evolution reaction remains practically unaltered, approaching the conditions observed in the early potential scans at $0.25\ V\ s^{-1}$ (see Fig. 1).

When $E_{s,a}$ is set close to the potential of Peak I, the returning cathodic potential excursion under STPS conditions exhibits a new cathodic current contribution (Peak V) at potentials just preceding the threshold potential of the hydrogen evolution reaction (Fig. 3). Current Peak I is assigned to the formation of the first passivating species, and the corresponding reaction is more clearly distinguished in still than in stirred solutions. Peak I appears as a single anodic contribution in the $0.001\ V\ s^{-1} < v < 10\ V\ s^{-1}$ range in the STPS run with still solutions. On the other hand, as v decreases Peak I exhibits a small pseudocapacitive current hump at *c.* − 0.6 V, which is probably related to the electro-oxidation of either molecular

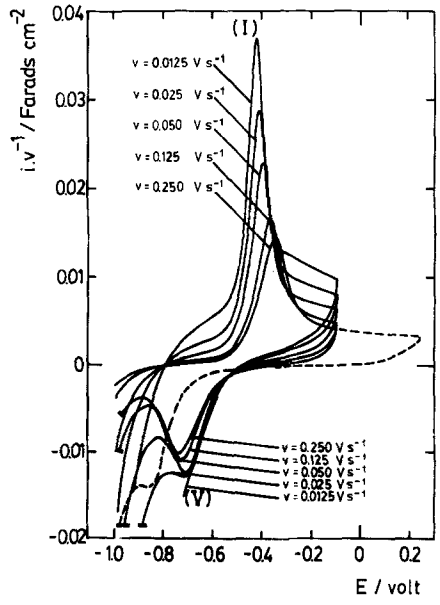

Fig. 3. STPS *E–I* displays run at different v between $E_{s,c} = -1.0$ V and $E_{s,a} = -0.1$ V with still solution. The dashed line corresponds to a run made at $v = 0.25\ V\ s^{-1}$ between $E_{s,c} = -1.0$ V and $E_{s,a} = 0.24$ V.

or atomic hydrogen. At a constant $E_{s,a}$ the location of Peak V becomes practically independent of v as the slight changes of the E–i contour are due to the contribution of the hydrogen discharge reaction. Otherwise, at constant v the greater $E_{s,a}$, the more negative the potential of Peak V ($E_{p,V}$) (see Fig. 3). This suggests that as $E_{s,a}$ increases anodic products exhibiting more efficient passivating properties are formed, so that the electrochemical reactions occurring afterwards can be regarded as processes of increasing irreversibility. The E–i profiles run at different v (see Fig. 3) also reveal two well defined isopotentials, at -0.79 and -0.53 V, respectively, just in the potential range associated with the Ni/Ni(OH)$_2$ electrode.

The E–i profile in the potential range of Peak I depends on the rotation speed ω (Fig. 4). Under stirring, at low v the first anodic excursion shows, at the positive potential side of Peak I, a new anodic process (Peak I'), whose relative contribution increases as v decreases. Therefore, the faradaic reaction associated with Peak I must also be considered as a complex process. This kinetic behaviour is, in principle, similar to that already found for the influence of ω on the active to passive transition at nickel in acid solutions containing sulphate ions [20–22]. In stirred solutions, at $v > 0.01$ V s^{-1}, Peak I results with a symmetry similar to that observed with still solutions. The characteristics of Peak V depend only on $E_{s,a}$.

Under a constant rotation speed the potential of Peak I ($E_{p,I}$) changes linearly with log v (Fig. 5),

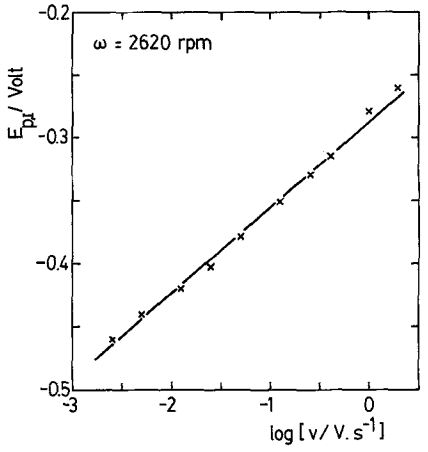

Fig. 5. Dependence of $E_{p,I}$ on v derived from STPS measurements. $\omega = 2620$ rpm.

the corresponding slope is 0.064 ± 0.007 V (decade)$^{-1}$, and the height of Peak I ($i_{p,I}$) fits a linear log $i_{p,I}$ vs log v relationship with a slope close to 1 (Fig. 6). These results can be correlated to those reported earlier in strong alkaline solutions [23, 24], indicating that the initial passivation process assigned to Peak I in carbonate electrolyte at pH 11.7 is essentially the same as that found in KOH solutions. From the STPS measurements carried out in the whole alkaline pH range, the following kinetic parameters for current Peak I can be derived:

$$(\partial \log i_{p,I}/\partial \text{ pH})_v = 0$$

and

$$(\partial E_{p,I}/\partial \text{ pH})_v = -0.06 \text{ V (decade)}^{-1}$$

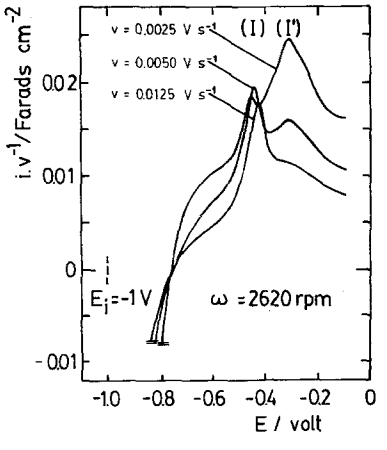

Fig. 4. STPS E–I displays run at low v and $\omega = 2620$ rpm.

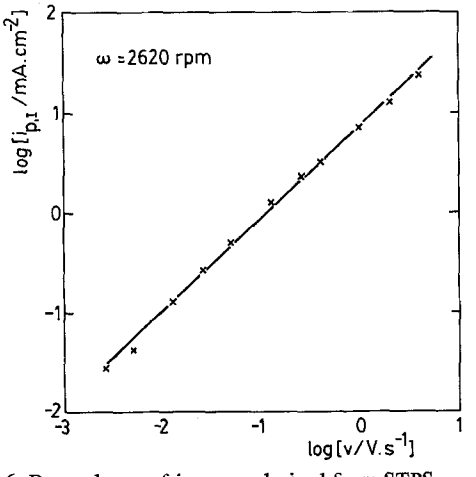

Fig. 6. Dependence of $i_{p,I}$ on v derived from STPS measurements. $\omega = 2620$ rpm.

Then, when the first anodic scan initiates from an $E_{s,c}$ value sufficiently negative to allow the complete electroreduction of the surface species remaining from the electrode pretreatment, the $Ni(OH)_2$ electroformation actually takes place on the bare metal. In this case, only the electrochemical reaction appears sufficiently simple to derive reproducible kinetic parameters for interpreting the reaction in terms of conventional mechanisms.

The stabilized potentiodynamic E–i profile resulting under steady electrode rotation is, in principle, similar to that previously described for the still electrolyte, although in the former case both $E_{p,II}$ and $E_{p,III}$ are shifted to more positive potentials. Nevertheless, in stirred electrolyte the charge accumulation in the potential range of Peaks II and III is smaller than in still electrolyte. This effect becomes clearer as v decreases. The RTPS E–i profile depends considerably on the perturbation characteristics and hydrodynamic conditions during the potential cycling, but the stabilized profile remains practically unaltered on further changes of ω. On the other hand, the relationships between the peak parameters and v are sensitive to the initial stabilization conditions of the interface. In the case for both Peaks II and III, any relationship between either E_p or i_p with v is of a rather limited value. Probably, the dependence of the different charge ratios with both v and ω becomes more relevant for discussing the kinetics of the reactions.

Peak IV which actually appears as a shoulder becomes more clearly resolved as $E_{s,a}$ increases. This result is also in agreement with those obtained for nickel in borate buffer solutions [13], although the charge contribution to the overall cathodic reaction is insensitive either to v or ω in comparable conditions.

4. Discussion

The potentiodynamic behaviour of nickel in potassium carbonate solutions is, to a great extent, qualitatively similar to that already observed in alkaline solutions and in buffered borate electrolyte, although in the former case there are some aspects which deserve further discussion.

The anodic process occurs in two parts, one in the -0.6–-0.2 V range which is related to the electroformation of the first passivating species, and another in the 0.5–0.9 V range which is associated with the complex Ni(II)/Ni(III) redox system. The initial passivation involves at least two processes, one is the formation of a thin $Ni(OH)_2$ hydrated layer and another the precipitation of a salt layer of either $NiCO_3$ or a basic nickel carbonate as should be expected from the pK_s value of $NiCO_3$ ($pK_s = 8.18$ at 25° C where s denotes solubility) [25]. This means that the anodic Peak I is composed of two passivation peaks, whose contribution actually depends on the charge playing part in the potential sweep, that is, on the potential scan rate. This can be put forward in terms of two reactions:

$$Ni + H_2O = Ni(OH)_2 + 2H^+ + 2e \quad (1)$$

and

$$Ni + CO_3^{2-} = NiCO_3 + 2e \quad (2)$$

Reactions 1 and 2 can be related to a competitive reaction mechanism given in terms of the electrooxidation reaction to Ni(II), such as:

$$\begin{array}{lll} & \xrightarrow{(2OH^-)} & Ni(OH)_2 \\ & & \uparrow\downarrow \\ Ni & \rightleftharpoons & Ni^{2+} + 2e \\ & & \uparrow\downarrow \\ & \xrightarrow{(CO_3^{2-})} & NiCO_3 \end{array} \quad (1a), (2a)$$

The formation of $Ni(OH)_2$ as is usually found in metal passivity by oxide layer formation, does not require supersaturation with respect to the electrolyte, but a potential exceeding that of Reaction 1. In contrast, $NiCO_3$ precipitation should occur once the Ni^{2+} ion concentration at the surface corresponds to at least saturation. As is already known in the literature [26], a supersaturation ratio of 1–5 times the saturation for precipitation of various metal salts has been calculated. Consequently, under the experimental conditions of any relaxation technique, the relative contribution of Reactions 1a and 2a should depend on the overall charge involved in the experiment. This explains how under a rapid potential scan and under solution stirring the contribution of Reaction 2a diminishes. Then, the first influence of CO_3^{2-} ions in the anodic process is to compete in the formation and stabilization of the prepassive layer. The charge playing part in the $Ni(OH)_2$ layer can be also estimated from that involved in the Ni(II)/Ni(III) redox couple. Therefore, at constant v as ω increases the fraction of charge which is anodized to Ni(III) in the potential range of Peak II decreases compared to that related to the Ni(II)

species electroformed in the potential range of Peak I. The same effect is observed at a constant ω as v decreases.

The cathodic reaction related to Peak V, corresponds to the electro-reduction of the $Ni(OH)_2$ fraction of the prepassive layer, as has been found for nickel both in acid and alkaline electrolytes [21, 23]. Furthermore, the $Ni(OH)_2$ layer also exhibits complex chemical and electrochemical behaviour as its composition appears to be considerably dependent upon the anodic switching potential reached during the potential sweep. In this case, it is likely that the degree of hydration of the oxo–hydroxide layer decreases as the potential increases, thus making the electro-reduction process more irreversible (see Fig. 3). Another consequence of the composition change of $Ni(OH)_2$ should also be reflected in the solubility of the anodic layer of the electrolyte, although in this case, due to the presence of CO_3^{2-} ions, the corresponding solubility should be conditioned by ionic equilibria such as:

$$|Ni(OH)_2|_{E_{s,a}} + CO_3^{2-} = NiCO_3 + 2OH^- \quad (3)$$

where $|Ni(OH)_2|_{E_{s,a}}$ denotes a hydrated $Ni(OH)_2$ layer formed during the potential sweep up to $E_{s,a}$ at preset perturbation conditions.

On the other hand, under rotation, when most of the reaction goes through the formation of $Ni(OH)_2$, the $i_{p,I}$ vs v and $E_{p,I}$ vs log v relationships approach the same values as those reported for nickel in KOH solutions ($0.01\ M < C_i < 1\ M$) which are consistent with the following reaction scheme already discussed in previous publications [15, 23]:

$$Ni(H_2O)_{ad} + OH^- \rightleftarrows Ni(OH)_{ad} + H_2O \quad (4)$$

$$Ni(H_2O)_{ad} \rightleftarrows Ni(OH)_{ad} + H^+ + e \quad (5a)$$

$$Ni(OH^-)_{ad} \rightleftarrows Ni(OH)_{ad} + e \quad (5b)$$

$$Ni(OH)_{ad} \rightleftarrows Ni(OH^+)_{ad} + e \quad (5c)$$

$$Ni(OH^+)_{ad} \rightleftarrows Ni^{2+} + OH^- \quad (5d)$$

$$Ni(OH)_{ad} + H_2O \rightarrow Ni(OH\cdot H_2O)_{ad} \quad (6)$$

$$Ni(OH\cdot H_2O)_{ad} \rightleftarrows Ni(OH)_2 + H^+ + e \quad (7)$$

where Step 6, which is a surface layer reaccommodation process, becomes, in this case, the rate determining step, and $Ni(OH)_2$ appears as hydrated species once the corresponding solubility product is exceeded.

From a direct comparison with the electrochemical behaviour of nickel in strong alkaline aqueous solutions current Peaks II, III and IV are related to the complex reaction [16, 27]

$$Ni(OH)_2 + OH^- \rightleftarrows NiOOH + H_2O + e \quad (8)$$

The gradual changes observed during the successive potential excursions and the drastic variation in shape of the current contributions related to Peaks II and III can be reasonably associated with the transformations of the surface species initially formed from either $Ni(OH)_2$ or NiOOH types [15]. These species undergo chemical changes to more stable configurations in coincidence with the interconversion reactions in strong alkaline electrolytes postulated earlier to interpret the non-equilibrium effects detected after a proper adjustment of the time scale of the perturbation programme [17, 27].

The influence of the solution composition is also reflected in the gradual change of the E–i profiles on cycling in the potential range of the redox Ni(II)/Ni(III) couples, including a part of the molecular oxygen evolution E–i profile, when the charge involved in the charging–discharging cycle corresponds to only a few layers of active material. As the number of scans increases the molecular oxygen evolution reaction becomes more irreversible and during the second potential sweep both the anodic and cathodic profiles exhibit a clear triplet. Finally, after prolonged cycling practically only Peaks II, III and IV are recorded. One interesting fact is the considerable contribution of Peak IV in the electro-reduction profile as compared to that observed with other electrolytes under the same perturbation conditions. This peak was attributed to the electro-reduction of γ_1-NiOOH [17, 28]. If the composition and structure of the hydrous layers is conceived as a hydrogen-bonded aggregate with a rather open structure, hydroxyl ions and water and the rest of the ions in solution should be part of the structure since they are required to minimize space charge effects within the layer. Therefore, ions may act in changing the defect structure of the NiOOH layer. The latter is expected to be significant as the charge transfer rate through the NiOOH lattice is quite likely to be determined by proton jump transport [29, 30]. Apparently

the discharge efficiency of γ_1-NiOOH is poor as it only undergoes substantial discharge at low rates [31, 32] but this efficiency seems to be increased in the borate electrolyte. The anion influence probably appears through the removal of Ni^{3+} or Ni^{4+} defects from the $Ni(OH)_2$ layer as the hydrated oxo–hydroxide layer is discharged towards the divalent state as already pointed out by Barnard *et al.* [33, 34].

The *E–i* profiles in the potential range of the Ni(III)/Ni(IV) redox couples are considerably influenced by the composition of the solution as compared to those resulting in sodium hydroxide and borate solutions at the same pH and ageing conditions [13, 17]. Thus, the splitting of the cathodic voltammogram is appreciably enhanced in carbonate solution, particularly the contribution of that related to the electro-reduction of γ_1–NiOOH [27, 35]. This can be tentatively explained as a change in the structure of the $Ni(OH)_2$–NiOOH film, particularly in the degree of hydration which operates with a greater degree of difficulty to lose protons in the anodic reaction yielding a relatively larger amount of γ_1–NiOOH and in the greater cathodic charge contribution in the corresponding electro-reduction reaction. This conclusion can be derived from the redox behaviour of hydrous nickel oxide films produced by potential cycling [12, 16, 27, 35–41]; as the prepassive film can be considered as a homogeneous mixture of simultaneously-formed hydrated $Ni(OH)_2$ and $NiCO_3$. Since the anodic reaction is a proton source while the cathodic reaction is a proton sink, it is probable that CO_3^{2-}; ions in the anodic layer participate in the equilibrium:

$$HCO_3^- = CO_3^{2-} + H^+ \qquad (9)$$

Thus anions involved in the reaction alter the hydrogen-bonded network of local water [42]. Hence the hydration of the anodic film is changed as well as the relative contribution of the different structures in the overall composition of the anodic layer [43].

Moreover, the influence of the solution composition should be shown in the growth rate of the anodic film, although its stability towards both open-circuit breakdown and electro-reduction depends on both the time and the potential of anodic film treatment [7, 9, 13]. This implies a homogeneous change in depth in the film composition [15], a structure which makes it difficult to draw reliable conclusions about the influence of pH on the redox behaviour of hydrous nickel oxide layers [40]. From a comparison of the electro-reduction charge of the anodic films it appears that in carbonate electrolyte thicker oxide films can be grown at potentials in the oxygen evolution potential region, as has been reported in borate electrolyte [9, 10, 13, 44].

Acknowledgements

The INIFTA is sponsored by the Consejo Nacional de Investigaciones Científicas y Técnicas, the Universidad Nacional de La Plata and the Comisión de Investigaciones Científicas (Provincia de Buenos Aires). This work was partially supported by the Multinational Chemistry Programme of the Organization of American States. One of us (A.E.B.) thanks CONICET for the fellowship granted.

References

[1] N. Sato, K. Kudo and M. Miki, *J. Jpn Inst. Metals* **35** (1971) 1007.
[2] N. Sato and K. Kudo, *Electrochim. Acta* **19** (1974) 461.
[3] B. MacDougall and M. Cohen, *J. Electrochem. Soc.* **121** (1974) 1152.
[4] J. L. Ord, J. C. Clayton and D. J. De Smet, *ibid.* **124** (1977) 1714.
[5] O. G. Deryagina and E. N. Paleolog, *Electrokhimiya* **14** (1978) 996.
[6] M. S. Abdel Aal and A. H. Osman, *Corrosion* **36** (1980) 591.
[7] B. MacDougall, D. F. Mitchell and M. J. Graham, *J. Electrochem. Soc.* **127** (1980) 1248.
[8] D. C. Silverman, *Corrosion* **37** (1981) 546.
[9] B. MacDougall and M. J. Graham, *J. Electrochem. Soc.* **128** (1981) 2321.
[10] C. Y. Chao, Z. Szklarska-Smialowska and D. D. Macdonald, *J. Electroanal. Chem.* **131** (1982) 279.
[11] *Idem, ibid.* **131** (1982) 289.
[12] L. D. Burke and T. A. M. Twomey, *J. Electroanal. Chem.* **134** (1982) 353.
[13] L. M. Gassa, J. R. Vilche and A. J. Arvía, *J. Appl. Electrochem.* **13** (1983) 135.
[14] J. R. Vilche and A. J. Arvía in 'Passivity of Metals', edited by R. P. Frankenthal and J. Kruger, The Electrochemical Society Inc., Princeton, (1978) pp. 861–77.
[15] *Idem* in 'The Nickel Electrode', edited by R. G. Gunther and S. Gross, The Electrochemical Society Inc., Pennington, (1982) pp. 17–47.
[16] R. S. Schrebler Guzmán, J. R. Vilche and A. J. Arvía, *J. Electrochem. Soc.* **125** (1978) 1578.
[17] H. Gómez Meier, J. R. Vilche and A. J. Arvía, *J.*

Appl. Electrochem. **10** (1980) 611.
[18] J. R. Vilche and A. J. Arvía, *Corros. Sci.* **15** (1975) 419.
[19] R. S. Schrebler Guzmán, J. R. Vilche and A. J. Arvía, *J. Appl. Electrochem.* **8** (1978) 67.
[20] J. R. Vilche and A. J. Arvía, *Corros. Sci.* **18** (1978) 441.
[21] S. G. Real, J. R. Vilche and A. J. Arvía, *ibid.* **20** (1980) 563.
[22] J. R. Vilche and A. J. Arvía, *J. Electrochem. Soc.* **123** (1976) 1061.
[23] R. S. Schrebler Guzmán, J. R. Vilche and A. J. Arvía, *Corros. Sci.* **18** (1978) 765.
[24] J. R. Vilche and A. J. Arvía, *Lat. Amer. J. Chem. Eng. Appl. Chem.* **9** (1979) 35.
[25] L. Meites (Ed.) 'Handbook of Analytical Chemistry', McGraw-Hill, New York (1963) pp. 1–17.
[26] W. Lorenz, *Z. Phys. Chem.* **20** (1959) 95.
[27] R. S. Schrebler Guzmán, J. R. Vilche and A. J. Arvía, *J. Appl. Electrochem.* **9** (1979) 183.
[28] R. E. Carbonio, V. A. Macagno, M. C. Giordano, J. R. Vilche and A. J. Arvía, *ibid.* **12** (1982) 121.
[29] D. M. MacArthur, *J. Electrochem. Soc.* **117** (1970) 422.
[30] *Idem, ibid.* **117** (1970) 729.
[31] J. P. Harivel, B. Morignat, J. Labat and J. F. Laurent, *Power Sources* **1** (1966) 239.
[32] D. Tuomi, *J. Electrochem. Soc.* **112** (1965) 1.
[33] R. Barnard, C. F. Randell and F. L. Tye, *J. Appl. Electrochem.* **10** (1980) 109.
[34] *Idem, ibid.* **10** (1980) 127.
[35] R. S. Schrebler Guzmán, J. R. Vilche and A. J. Arvía, *ibid.* **9** (1979) 321.
[36] H. Bode, K. Dehmelt and J. Witte, *Z. Anorg. Allgem. Chem.* **366** (1969) 1.
[37] H. Bartl, H. Bode, G. Sterr and J. Witte, *Electrochim. Acta* **16** (1971) 615.
[38] G. W. D. Briggs and M. Fleischmann, *Trans. Faraday Soc.* **67** (1971) 2397.
[39] G. W. D. Briggs and P. R. Snodin, *Electrochim. Acta* **27** (1982) 565.
[40] L. D. Burke, M. E. Lyons, E. J. M. O'Sullivan and D. P. Whelan, *J. Electroanal. Chem.* **122** (1981) 403.
[41] M. E. Folquer, J. R. Vilche and A. J. Arvía, *J. Electrochem. Soc.* **127** (1980) 2634.
[42] M. I. Sosa and A. J. Arvía, *An. Acad. Cs. Ex. Fis. Nat.* (Buenos Aires) **34** (1982) 153.
[43] P. Oliva, J. Leonardi, J. F. Laurent, C. Delmas, J. J. Braconnier, M. Figlarz and F. Fievet, *J. Power Sources* **8** (1982) 229.
[44] A. E. Bohé, L. M. Gassa, J. R. Vilche and A. J. Arvía, Proceedings of the IIIrd Brazilian Symposium on Electrochemical Electroanalysis', Sao Carlos, 5–7 April, 1982, pp. 111–6.